Autonomous Object Manipulation using a Soft Planar Grasping Manipulator

Robert K. Katzschmann, Andrew D. Marchese, and Daniela Rus*

October 16, 2015

Abstract

This paper presents the development of an autonomous motion planning algorithm for a soft planar grasping manipulator capable of grasp-and-place operations by encapsulation with uncertainty in the position and shape of the object. The end effector of the soft manipulator is fabricated in one piece without weakening seams using lost-wax casting instead of the commonly used multi-layer lamination process. The soft manipulation system can grasp randomly positioned objects within its reachable envelope and move them to a desired location without human intervention. The autonomous planning system leverages the compliance and continuum bending of the soft grasping manipulator to achieve repeatable grasps in the presence of uncertainty. A suite of experiments is presented that demonstrates the system's capabilities.

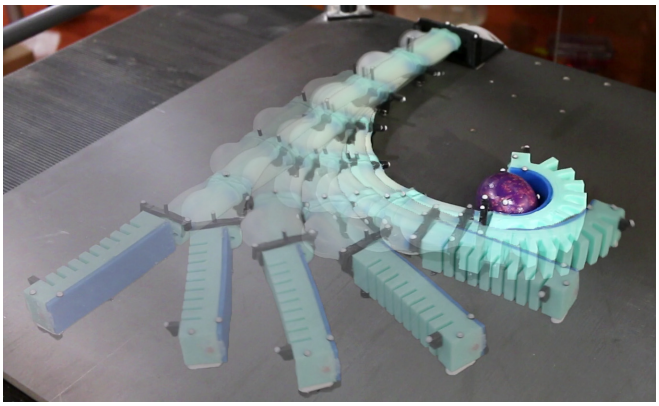

Figure 1: The soft manipulator is grasping an egg. The robot repeatably approached, grasped and moved this delicate object without breaking it.

1 Introduction

Soft robots exhibit continuum body motion, large scale deformation, high compliance, and adjustable impedance compared to traditional rigid-bodied robots with high impedance [24].

Such characteristics make this class of robots well-suited for highly dexterous tasks and interactions that require conformation to environmental uncertainty.

Our goal is to develop a soft planar fluid-powered gripper and a motion planning algorithm that leverages a soft morphology to robustly grasp, drag, and place objects of unknown geometry. In this paper we describe a planar soft robot manipulator we developed toward this goal. We focus on the design, fabrication, control, and planning aspects of this soft robot.

The fluid-powered gripper at the end of the arm can grasp an object through an open-loop controlled bending motion, even if the gripper is positioned relatively inaccurately in relation to the object to be grasped. The design of the gripper itself is inspired by the work of Polygerinos et al. [19] The design is advantageous for grasping, because it exhibits high curvature, minimal radial expansion, and remains compliant during actuation. We can repeatably fabricate the gripper using a lost-wax casting process instead of the commonly used soft lithography technique.As a homogeneous piece without weakening seams, the gripper is not prone to de-lamination under high deformations. By abandoning the need for a lamination process, arbitrary shaped internal channels can be achieved.

We attach the gripper to a multi-segment soft manipulator to enable autonomous grasp-and-place capabilities on a plane. Positional feedback is provided in real-time from a camera system. Modeling uncertainties arise from a simplifying constant-curvature assumption, unrepresented manipulator dynamics, stick-slip friction, and non-linear fluidic control. These uncertainties are compensated by the inherent compliance of our soft gripper design and our motion planning strategy. The motion planning algorithm advances the arm through all the necessary states of the grasp-and-place operation. A minimal strain, collision-free movement towards the object of interest is found by posing the plan as a series of constrained nonlinear optimization problems. The system first plans concentric approach circles shrinking from the initial end-effector pose down to the object diameter. Next, the system searches for locally optimal manipulator configurations that constrain the end-effector to lie on these approach circles, so that the manipulator does not collide with the object. The manipulator is then moved between these plans using closed-loop trajectories. After successfully approaching the object, the gripper encapsulates it. Even when the arm and gripper are fully actuated, they remain compliant allowing it to conform to un-modeled object geometries. We experimentally validate the system's

*Robert K. Katzschmann, Andrew D. Marchese, and Daniela Rus are with the Computer Science and Artificial Intelligence Laboratory, Massachusetts Institute of Technology, 32 Vassar St. Cambridge, MA 02139, USA, rkk@csail.mit.edu

ability to repeatably and autonomously grasp-and-place randomly placed objects.

1.1 Related Work

An overview of soft robotics is presented in Rus and Tolley [20]. We will cover in the following the relevant works in fabrication, grippers and control of soft robots.

Several manufacturing processes for soft biomimetic robots were reviewed by Cho et al. [5]. The vast majority of soft elastomer robots rely on the processes of soft lithography [26] and/or shape deposition manufacturing [4]. Especially noteworthy is the use of wax for fabricating jammable skin chambers, which stiffens by vacuuming [22]. The gripper presented in this work also uses a lost-wax molding technique, but with a different type of actuation in mind: the obtained cavity structures are inflated to cause the gripper to bend.

There are several hardware examples for soft grippers described in recent literature, we will mainly focus on fluidic-based systems. Deimel and Brock [6] developed a pneumatically actuated three-fingered hand made of reinforced silicone that is mounted to a hard robot and capable of grasping. More recently, they have developed an anthropomorphic soft pneumatic hand capable of dexterous grasps, which is not mounted to a robot, but instead held by a human [7]. Using a soft-lithography fabrication, Ilievski et al. [11] created a pneumatic starfish-like gripper composed of an array of silicone chambers and a PDMS membrane. The gripper hangs on a string and grasps objects like an egg or a mouse in an open-loop controlled manner. Stokes et al. [23] use a soft elastomer quadrupedal robot attached to a wheeled robot to grip and retrieve objects. A puncture resistant soft pneumatic gripper is developed by Shepherd et al. in [21]. An alternative to positive pressure actuated soft grippers is a robotic gripper that makes use of granular material jamming developed by Brown et al. and detailed in [1]. Ikuta and Suzuki [10] demonstrated a multiple-segment micro-hydraulic actuator for entering blood vessels. The soft octopus-inspired arms developed in [2] and [3] are not fluidic powered, but instead use cables to pull rigid fixtures embedded within an elastomer body. The arms were capable of grasping objects like pens or screws. A soft robotic tentacle developed in [17] was able to hold a flower and a horseshoe-shaped object. The closest related soft pneumatic actuator design to our current work is the fast Pneu-net designs by Mosadegh et al. [18] and by Polygerinos et al. [19]. These finger-like actuators deform with minimal volume change and can bend to high curvatures. None of the above described grippers were controlled autonomously to perform their tasks and accordingly no statement on repeatability of the autonomous execution was given.

Simulation results using an online motion planner for a planar continuum manipulators were presented by Xiao and Vatcha[27]. This work was extended by Li and Xiao [13] to present a more general formulation to constrained, continuum manipulation. Marchese et al. [16] demonstrated closed-loop position control of a multi-segment soft planar fluidic elastomer manipulator in free space. The soft manipulator presented in [14] is only suitable for inspection tasks by moving through a constrained environment without object interaction or manipulation.

The work presented here combines two soft actuator types to leverage their strengths in a planar manipulation task. A new control method described here demonstrates the capabilities of this new soft manipulator to perform autonomous manipulations with uncertainties.

1.2 Contributions

We take on the challenge of grasping-and-placing objects with a seven degrees of freedom planar arm made entirely from soft rubber. Our work differs from the previous work in that we create an entirely soft and autonomously controlled *grasping* manipulation system. Our planning and control method successfully copes with uncertainties in the object geometries, object placement and manipulator modeling. We provide in this work the following contribution to soft robotics:

- The design and fabrication process of a soft 2D manipulator.
- A planning algorithm to grasp-and-place randomly positioned objects on a planar surface using a 7 DOF soft manipulator.
- Autonomous manipulation experiments with various objects of unknown geometry placed randomly in the working space of a soft manipulator without requiring force sensing or accurate positioning.
- Data from repeatable successful grasping demonstrations with a physical prototype and a qualitative experimental characterization of the uncertainty regions that can be tolerated by the soft gripper.

2 System Overview

The soft grasping manipulator shown in Figure 1 has six bidirectional segments with cylindrical cavities forming the arm and a single soft gripper with a pleated shape (Figure 2) as the end effector. The independent pneumatic actuation of the unidirectional soft gripper and each bidirectional arm segment, is achieved through an array of 13 custom fluidic drive cylinders [16]. An object of feasible size but unknown geometry is randomly placed within the reachable envelop of the manipulator. The location of the manipulator and the object is determined with an external localization system. The motion planning algorithm as well as the curvature controller run on the control computers and take the location information as input. The curvature controller then provides continuous closed-loop adjustment of the fluidic drive cylinder array.

3 Soft Grasping Manipulator

The robotic manipulator is composed of multiple bidirectional planar arm segments and combined with a unidirectional soft

gripper. We briefly describe the design, fabrication and functionality of this soft grasping manipulator in this paper. Further details on the design and fabrication can be found in [15].

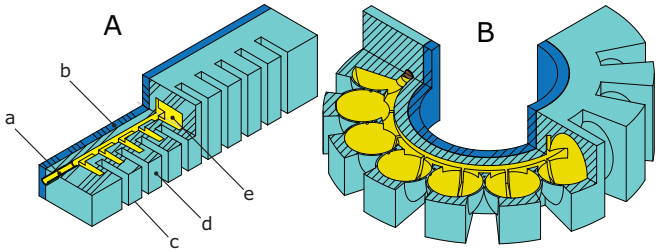

Figure 2: The pleated channel designs. The design consists of a channel inlet (a), an almost inextensible constraint layer (b), uniform pleats (d) separated by even gaps (c), and internal channels within each pleat (e). (**A**) depicts the segment in an unactuated state and (**B**) shows the segment in an actuated and therefore bent state. The expansion of the pressurized channels are schematically represented. Reproduced from [15].

3.1 Pleated Channel Design for the Gripper

The pleated channel design consists of evenly spaced ribs shown in *cyan* with embedded hollow sections shown in *yellow*. Cut views of the un-actuated and actuated states are shown in Figure 2. This design approach draws inspiration for its pleats from the soft pneumatic gloves developed by Polygerinos et al. [19] and its homogeneous body design is inspired from the tail design of a soft robotic fish developed by Katzschmann et al. [12]. This design is advantageous for grasping because it exhibits high curvature, minimal radial expansion, and remains compliant during actuation [15]. The hollow ribs within the segment's pleats are connected by a center channel and are accessible through a front inlet. Under fluidic pressurization of the interior channel, an individual pleat allows for a ballon-like expansion of the thin exterior skin along the axial direction. Similar to the uniform channel design, a stiffer silicone layer shown in *blue* serves as an almost inextensible constraint layer. The sum of the ballon-like expanding motions leads to bending of the less extensible center constraint layer to form a grasp. The pleated design is capable of unidirectional bending up to extreme curvatures. Using a lost-wax casting approach, we are not limited in defining the geometry of the segment's fluidic channels. Using this approach, the *cyan* portion of the pleated gripper can be cured in a single step, avoiding any weakening seams due to lamination.

3.2 Lost Wax Fabrication for Fluidic Elastomer Actuators

Existing soft fluidic manipulators are mostly produced through a multi-step lamination process called *soft lithography*, which results in weakening seams that can easily delaminate. This limits their range of applications and lifetime. The retractable pin fabrication for uniform lateral channels, first introduced in [14], limits the complexity of the cavities to cylindrical shapes but does not cause weakening seams to the actuator. This is why the application of lost-wax casting to the fabrication of soft fluidic actuators like a gripper is advantageous. The actuated cavities of the soft gripper are achieved using a wax core, pourable silicone rubber and 3D printed molds. The gripper fabrication process and the tools needed are fully described and depicted in Section 4.3. and Figure 14 in [15].

3.3 Multi-segment Arm with Gripper

The design for the arm consisting of soft cylindrical segments is described in [14]. As is shown in [15] through the characterization of various actuator morphologies, the concatenation of soft cylindrical segments is most suitable to build up a robotic arm that can create high blocking forces per fluid energy inserted. The cylindrical segments of the arm are fabricated through a retractable pin fabrication technique [14], which does not require lost wax cores because of their simple cylindrical cavities. Each cylindrical segment can be actuated up to a bend angle of about $60°$, this requires several segments to be combined together to allow the arm to reach a large enough workspace to perform proper manipulation tasks on a plane. Using six segments, the robot is able to touch its tip to its base without interference from the individual joint limits. The cylindrical segment design with its hollow channel in the center has enough space to accommodate for pneumatic tubes to connect to all six cylindrical segments and additionally to the pleated gripper, which is attached to the tip. The pleated gripper has to be appropriately sized, just big enough to allow for proper manipulation without exceeding the payload capacity of the soft arm.

The complete multi-segment arm is supported off the ground with two roller supports per segment. The rollers minimize frictional forces to the surface. If the arm would be moved over a non-slippery surface without rollers, the frictional effects would greatly reduce the agility of the arm and largely increase the stick-slip friction effects with the ground, rendering the arm less useful.

4 Planning and Control

This section covers our approach to preplanning motion waypoints for the soft robot and controlling the manipulator along those points.

4.1 Kinematic Control

The forward kinematics algorithm `forwKin()` assumes piece-wise constant curvature [25]. In order to uniquely fit a configuration representation to measured endpoint data in real-time, we use a previously developed single segment inverse kinematics algorithm `singSegInvKin()` [16]. The inputs to this block are the start and endpoint measurements in $\mathbb{R}^2$: $\mathbf{E}_n \ \forall n = 1..N$, where N is the number of segments composing

the arm. The outputs from this block are the representations of the measured manipulator configuration: measured curvature $\boldsymbol{\kappa}_{\text{meas}}$ and segment length $\mathbf{L}_{\text{meas}}$. A cascaded closed-loop curvature controller `curvatureController()` takes the target curvatures $\boldsymbol{\kappa}_{\text{target}}$ as its input and resolves the error between $\boldsymbol{\kappa}_{\text{target}}$ and $\boldsymbol{\kappa}_{\text{meas}}$ by continuously adjusting the fluidic drive cylinder array.

We build on the path planning algorithm presented in [14]. This prior work plans the motion of a soft arm without a gripper through a maze at a centerline while taking the arms bulging shape into account. The approach does not work for approaching and grasping objects, since a tip trajectory for successfully moving towards the object is not known, but needs to be generated by posing and solving a new optimization problem. The manipulator trunk should not push the object away when approaching it. Therefore, a new planner had to be developed and is presented in the following section.

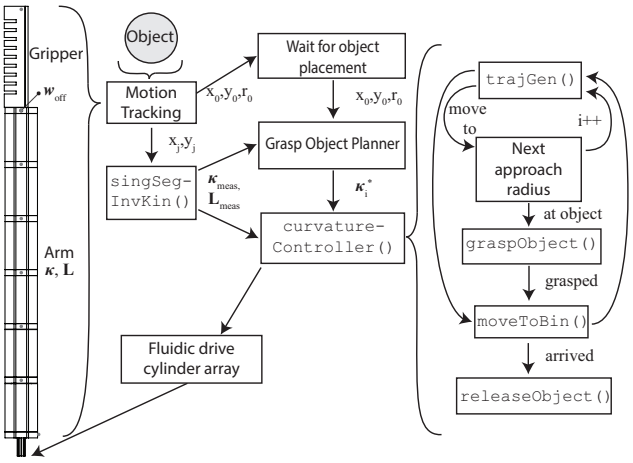

Figure 3: State flow diagram of the planner developed for the autonomous grasp-and-place operation of the manipulator. This diagram describes essentially the flow of information from the motion tracking system to the discrete hardware.

4.2 Autonomous Grasp-and-Place System

The robotic manipulation system is capable of autonomously performing grasp-and-place operations. A state flow diagram describing its sensing, planning and executions states is given in Fig. 3. A motion tracker constantly captures the position of the object. The Grasp Object Planner receives the coordinates and radius of the object and together with the current curvature values of the arm and gripper, it solves a series of constrained nonlinear optimization problems to generate end-effector poses approaching the object. Those end-effector poses are waypoints for an optimized path the robot arm should take to get to the final position without the risk of moving the object before the gripper grasps it. The intermediate waypoints ensure that the arm moves to the object while its null space maintains a convex shape, always bending away from the object. This is a conservative approach for not prematurely colliding with the object. Furthermore, this approach allows the arm to move in smaller steps, decreasing the risk of large overshoots due to slip-stick friction between the roller supports and the ground. This planner is described in more detail in Section 4.3.

The Grasp Object Planner passes the approach configurations $\boldsymbol{\kappa}_i^*$ of the arm to the `curvatureController()` for execution in real-time. The controller receives measured curvatures $\boldsymbol{\kappa}_{\text{meas}}$ and lengths $\mathbf{L}_{meas}$ at an update rate of 100 Hz from the recursively called `singSegInvKin()` and uses them to successively control the arm to every intermediate configuration $\boldsymbol{\kappa}_i^*$. During the arm initialization, the new curvature controller performs a pre-pressurization of both lateral channels. This is only done for the two segments closest to the root of the arm in order to stiffen them and shorten their response time constant. To allow for smoother transitions between each configuration $\boldsymbol{\kappa}_i^*$, we also added a trajectory generation procedure `trajGen()` to the new curvature controller. It generates in real-time velocity profiles with acceleration and velocity constraints for each individual degree-of-freedom. These profiles allow real-time interpolation between the approach configurations of the arm while avoiding overshooting at the next target configuration. When the arm has arrived at the desired pose next to the object, the curvature controller initiates `graspObject()`. After encapsulating the object, `moveToBin()` requests `trajGen()` for another trajectory from the current pose to a pre-defined bin location. When the manipulator gets close to the bin location, the procedure `releaseObject()` causes the gripper to open and release the object.

4.3 Grasp Object Planner

The grasp-and-place system plans a feasible approach motion to the object. That is, given the location (x_o, y_o) and radius r_o of a cylinder enclosing the object as well as the manipulator's current configuration $\boldsymbol{\kappa}_{\text{meas}}$ and segment lengths $\mathbf{L}_{\text{meas}}$, we determine a series of locally optimal manipulator configurations called approach configurations $\boldsymbol{\kappa}_i^* \ \forall i = 1..numMoves$ that will, if sequentially achieved, bring the manipulator gradually closer to the object while any part of the arm is not touching the object.

The process for determining the approach configurations is detailed in the `planGrasp()` procedure within the Grasp Object Planner, see Algorithm 1. The planner is visualized in Figure 4. In short, we define a series of approach radii $r_{a_i} \ \forall i = 1..numMoves$ that define concentric circles shrinking from the manipulator's starting tip pose towards the center of the object. Given actuator limits, we then search for a series of feasible manipulator configurations $\boldsymbol{\kappa}_i^*$ that will place the robot's end-effector on the approach circles, parameterized by r_a and ϕ, while minimizing manipulator deformation. Minimized manipulator deformation is chosen as the optimization criterion, because it is proportional to the energy consumed by the fluidic drive cylinders and it also minimizes the strain to the soft actuators.

The procedure `planGrasp()` in Algorithm 1 first determines the manipulator's current tip pose $\mathbf{w}_t$ and the Euclidean

Algorithm 1: Grasp Object Planner

Input: $\boldsymbol{\kappa}_{\text{meas}}, \mathbf{L}_{\text{meas}} \leftarrow$ measured arm configuration
$\boldsymbol{\kappa}_{\text{off}} \leftarrow$ measured manipulator configuration at start
$g_{\text{off}} \leftarrow$ gripper offset normal to end-effector
$x_o, y_o, r_o \leftarrow$ object center coordinates and radius
$N \leftarrow$ number of manipulator segments

Procedure `planGrasp()`

$\mathbf{w}_t \leftarrow$ `forwKin` $(\boldsymbol{\kappa}_{\text{meas}}, \mathbf{L}_{\text{meas}}, N, L_N)$.
$d_1 \leftarrow \| [x_o, y_o]^{\mathrm{T}} - \mathbf{w}_t \|$.
$d_2 \leftarrow d_1 - r_o - g_{\text{off}}$.
$numMoves \leftarrow \lfloor \frac{d_2}{\Delta d} \rfloor$.
$i = 0$.
repeat
  $i = i + 1$.
  $r_{a_i} \leftarrow d_1 - i \frac{d_2}{numMoves}$.
  $\boldsymbol{\kappa}_i^* \leftarrow$ `findOptimalConfig` (r_{a_i}).
until $i = numMoves$
return $\boldsymbol{\kappa}_i^* \quad \forall i = 1..numMoves$

Procedure `findOptimalConfig` (r_{a_i})

$$\boldsymbol{\kappa}^* \leftarrow \min_{\phi, \boldsymbol{\kappa}} \ \mathbf{R}\,(\boldsymbol{\kappa} - \boldsymbol{\kappa}_{\text{off}})^2.$$

subject to
$$\mathbf{w}_t \leftarrow \begin{bmatrix} x_o + r_{a_i}\cos\phi \\ y_o + r_{a_i}\sin\phi \\ \phi + \frac{\pi}{2} \end{bmatrix}.$$
$$\mathbf{f} \leftarrow \texttt{forwKin}\,(\boldsymbol{\kappa}, \mathbf{L}, N, L_N).$$
$$\mathbf{w}_t - \mathbf{w}_{\text{off}}\,(r_o, \phi) - \mathbf{f} = \mathbf{0}.$$
$$\kappa_n^{\min} \le \kappa_n \le \kappa_n^{\max} \quad \forall\, n = 1\,..\,N.$$

return $\boldsymbol{\kappa}^*$

Procedure `forwKin` $(\boldsymbol{\kappa}, \mathbf{L}, i, s)$

Input: $\boldsymbol{\kappa}$, $\mathbf{L}$, i the segment of interest index, s the arc length along the indexed segment
if $i = 0$ **then**
  $\theta_i(0) \leftarrow \theta_0(0)$.
  $x_i(0) \leftarrow 0$.
  $y_i(0) \leftarrow 0$.
else
  $[x_i(0), y_i(0), \theta_i(0)] \leftarrow$ `forwKin` $(\boldsymbol{\kappa}, \mathbf{L}, i-1, L_{i-1})$.
end
$\theta \leftarrow \theta_i(0) + k_i s$.
$x \leftarrow x_i(0) + \frac{\sin\theta}{k_i} - \frac{\sin\theta_i(0)}{k_i}$.
$y \leftarrow y_i(0) - \frac{\cos\theta}{k_i} + \frac{\cos\theta_i(0)}{k_i}$.
return $[x, y, \theta]^{\mathrm{T}}$ *or* $[x, y]^{\mathrm{T}}$

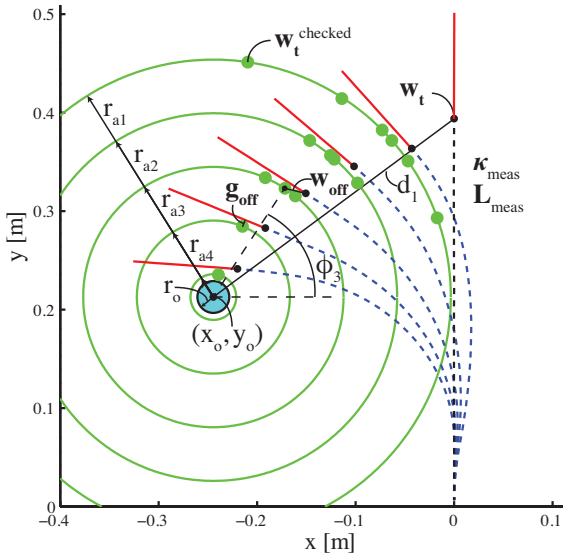

Figure 4: Visualization of the Grasp Object Planner. Concentric approach circles are centered about the object. The locally optimal approach configurations of the arm are shown as curved dashed lines with a straight gripper at the end. The initially measured manipulator configuration is shown as a long and dashed straight line on the right.

distance d_1 between the tip and the object's center. The arc length input to the arm's forward kinematics is the N-th element of the segment lengths $\mathbf{L}_{\text{meas}}$. The end effector offset $\mathbf{w}_{\text{off}}$ describes the distance from the root of the gripper to an offset point close to the lower end of the gripper's palm. It is visualized in the top left corner of Fig. 3. The length $\mathbf{g}_{\text{off}}$ represents the component of the end effector offset $\mathbf{w}_{\text{off}}$, which is normal to the end effector orientation. The minimal tip transit distance d_2 is calculated by considering the object's radius r_o and the gripper normal offset $\mathbf{g}_{\text{off}}$. Also, the number of approach configurations $numMoves$ is determined as $\lfloor \frac{d_2}{\Delta d} \rfloor$, where Δd is an allowable incremental distance. Using these parameters, approach radii r_a shown by the green circles are iteratively calculated and their corresponding locally optimal configurations are found by using the optimization equation and constraints described in procedure `findOptimalConfig` (r_{a_i}) of Algorithm 1.

The procedure `findOptimalConfig` (r_a) is posed as a nonlinear optimization problem. Here, the objective function represents the summation of independently weighted manipulator curvatures $\boldsymbol{\kappa} - \boldsymbol{\kappa}_{\text{off}}$. The weights are set by the matrix $\mathbf{R}$. The variables to optimize for are ϕ and κ. The optimization constraints cause the manipulator's tip to lie on and to be tangent to the approach circle. The constraints also ensure that the manipulator segment curvatures do not exceed the single soft actuator limits. Furthermore, this procedure leverages the arm's forward kinematics `forwKin()` defined in [16] and reproduced in the last section of Algorithm 1 for convenience. The optimization becomes over-constrained only if it has to find an arm pose outside of the arm's reachable workspace. That occurs if the object was user-placed out-

side the workspace. Before performing the optimization, a feasability check is performed using the arm's forward kinematics.

The nonlinear optimization problem is implemented on a PC using Sequential Quadratic Programming, which finds iteratively the minimum of a constrained nonlinear multivariable function. The solver is run with a relative upper bound of 2×10^{-3} on the magnitude of the constraint functions. The lower bound on the size of a step was given by 1×10^{-6}. The solver takes about $1\,\mathrm{s}$ to solve for all waypoints from start to finish.

5 Experimental Results

We now discuss the grasping of objects as well as the repeatability and success rate of the autonomous system.

5.1 Experimental Platform

The soft manipulation system we developed for this work is shown in Figure 5. Each arm segment is $6.27\,\mathrm{cm}$ and the soft gripper is $10.6\,\mathrm{cm}$ long. The localization system OptiTrack Flex 3 by Natural Point provides real-time measurements of marked points both along the inextensible back of the manipulator and on top of the object. A rigid frame holds all the subsystems as a mobile presentation platform together providing reliable hardware experiments without the need for recalibration.

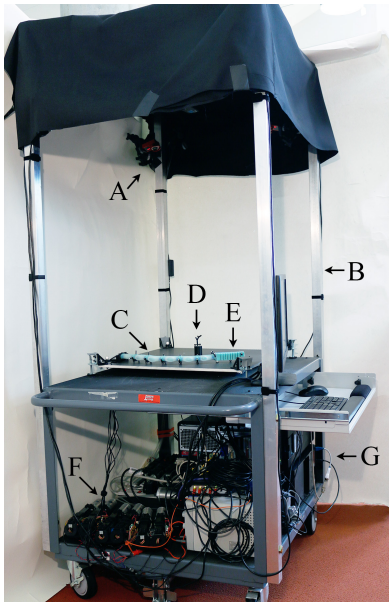

Figure 5: System Overview. The system is composed of (**A**) a motion capture system, (**B**) rigid frame, (**C**) soft six segment planar manipulator, (**D**) an object within the grasp envelope, (**E**) a soft gripper fixed to the manipulator, (**F**) a fluidic drive cylinder array to control actuation, and (**G**) computers for real-time processing and control.

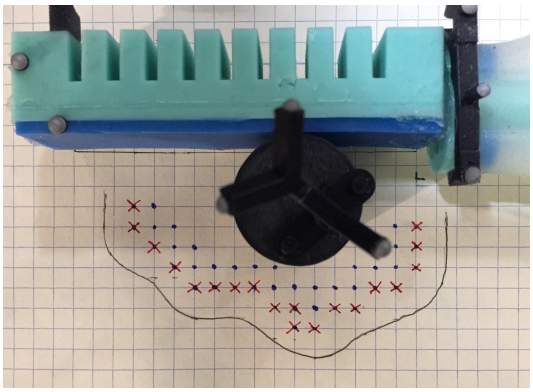

Figure 6: Experimental characterization of the gripper's capture region: the allowable positioning uncertainty is determined through repeated placements of the center of a cylindrical object at different points on a $5\,\mathrm{mm}$ grid relative to the gripper. Blue dots indicate all object center positions for which a grasp could be performed successfully, red crosses show the positions where a grasp failed. The grey line outlines an area for the object to be positioned within so the gripper can grasp it. The evaluation of the capture region was performed similarly to a method described in [8].

5.2 Grasp Experiments

Using the experimental platform in Figure 5, we implemented the planning algorithm described in Section 4. We evaluated the manipulator system for repeatability and ability to handle uncertainty. The experiments consisted of picking and placing several objects of unknown geometry placed at an unknown location. We measured the execution time and captured the location data during the experiments. Specifically, we performed over 200 experimental grasp-and-place trials at randomly chosen positions within the reachable workspace to demonstrate the capabilities and repeatability of our system. We successfully picked up various objects such as eggs, shuttlecocks, bakery items, cups, light bulbs, and tape holders. The objects had an enclosing diameter in the range of 2-5 cm. The results of a subset of those experimental trials are shown in Figure 7. One representative approach, grasp, and retract move is shown in Figure 8. In 23 of 25 experimental trials shown, the manipulator successfully achieved the task of grasping an object and placing it at a bin location shown in red. The test object has a weight of $18\,\mathrm{g}$ and a diameter of $3.3\,\mathrm{cm}$. The object was placed five times on each of the five points marked on the board. The markers only serve as a reference point for the user to place the object roughly at the same point at every repetition. The user's placing accuracy is not important to the algorithm, since the tracking system re-registers the position of the object every time it is placed. The five points were chosen to approximately represent the major portion of the manipulator's reachable workspace. As long as the root of the gripper stops so that the object is located within the capture region, the gripper will pick it up through its sweeping closing motion. The capture region is outlined in grey in Figure 6.

The evaluation of the capture region is performed simi-

larly to a method described in Dogar and Srinivasa[8] work on determining capture regions for a push-grasp of a classical robotic gripper. Grid paper and fine markings on all four sides of the round object ensure that the placement by the user is accurate within $\pm 1\,\mathrm{mm}$ in relation to the discrete placement locations on the grid. This test serves as a qualitative measure to show qualitatively a relation between object size to gripper size to area of successful grasp. This characterization was repeated two times, resulting in nearly identical capture regions. Despite positioning inaccuracies of the soft manipulator, the gripper can nevertheless successfully perform a grasp of an object. The successful capture region can be characterized by about half a gripper length in diameter.

When the arm reaches its straight pose within a relatively large delta, it drops the object. For these experiments, we focus on showing the capability of picking up objects at various places and moving them around, there is no emphasis set on having to drop off the object at a specific place. To indicate that the arm can move the object after grasping, the arm was controlled to go back to the fully straight pose. When the arm reached the final straight pose within a $1\,\mathrm{cm}$ delta, the gripper was set to release and drop the object. It was not ensured by the planner that the arm had to first settle to zero velocity at the final straight pose. As a consequence of this, the experimental data indicates as a red bin a relatively wide drop off area.

The unsuccessful trials happened due to stick-slip friction between the roller bearings and the table surface. Our kinematic modeling does not account for this non-linear behavior, which acts as a disturbance and can lead to failure to arrive at the next waypoint.

5.3 Experimental Insights and Limitations

Overall, the experiments show that the system was repeatably able to autonomously locate a randomly placed object within its workspace, plan the arm motions, and perform the task of grasping and placing the object. The system can drag payloads of less than $40\,\mathrm{g}$, higher payloads cause the cylindrical arm segments to stall and possibly lift off the table without moving the payload. There is a trade-off between the reachable workspace and the maximum payload. As the length of the arm increases, more workspace can be reached while less payload can be manipulated. A smoothing of the complete trajectory with several intermediate waypoints was found to be necessary. The amount of intermediate waypoints is determined by the variable Δd, which we found to be about the length of one arm segment.

We developed an end-to-end system that can approximately locate an object placed at an a priori unknown location and move it to a desired location. The external localization system is a convenient way to approximately identify the location of the object and to track how the object is moved around. The exteroceptive tracking system has the disadvantage that the full occlusion of one or more markers can cause the tracking system to temporarily loose track of a measured arm segment. In that case, the control loop can not function properly until the occlusion disappears. The external localization system could be replaced with another method for localizing the manipulator and the object in the workspace. For example, proprioceptive sensors within the segments could solve this issue partially. A first step towards proprioceptive sensing was done for three soft fingers arranged as a hand in [9].

The experiments were performed for picking up objects on the left quadrant of the manipulator. Grasping objects on both sides of the manipulator could be achieved in various ways including

1. replacing the large gripper at the end of the arm with two smaller grippers next to each other,
2. mounting roller supports on the top face of the manipulator and then rotating the manipulator at its root by 180°,
3. increasing the reachable workspace through starting the soft arm at an extreme curvature configuration within the right quadrant.

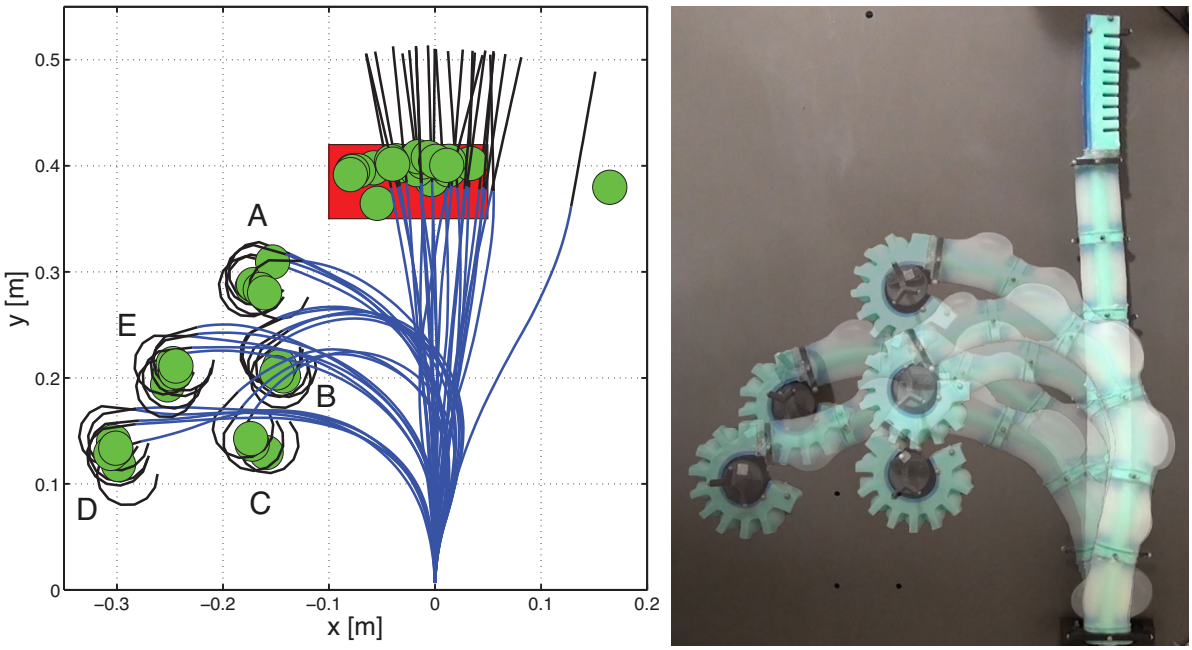

Figure 7: Left: Complete set of experimental grasp-and-place trials. In these experiments, the arm moves from an initial straightened configuration to grasp a round object placed in one of five locations (A-E). The arm then returns the object to a bin location shown in red. For each trial, a seven degrees of freedom manipulator representation is generated at both the *grasped* and *released* state using experimental data and is shown in blue. The corresponding 1 DOF end-effector representation is shown in black. The round object's measured position at each state is shown in green. In one of the trials, the grasp and return was successfully performed, but an overshoot over the final bin location caused the gripper to drop off the small table it is moving on. Right: Overlaid photographs of the manipulator grasping an object placed at each of the five locations.

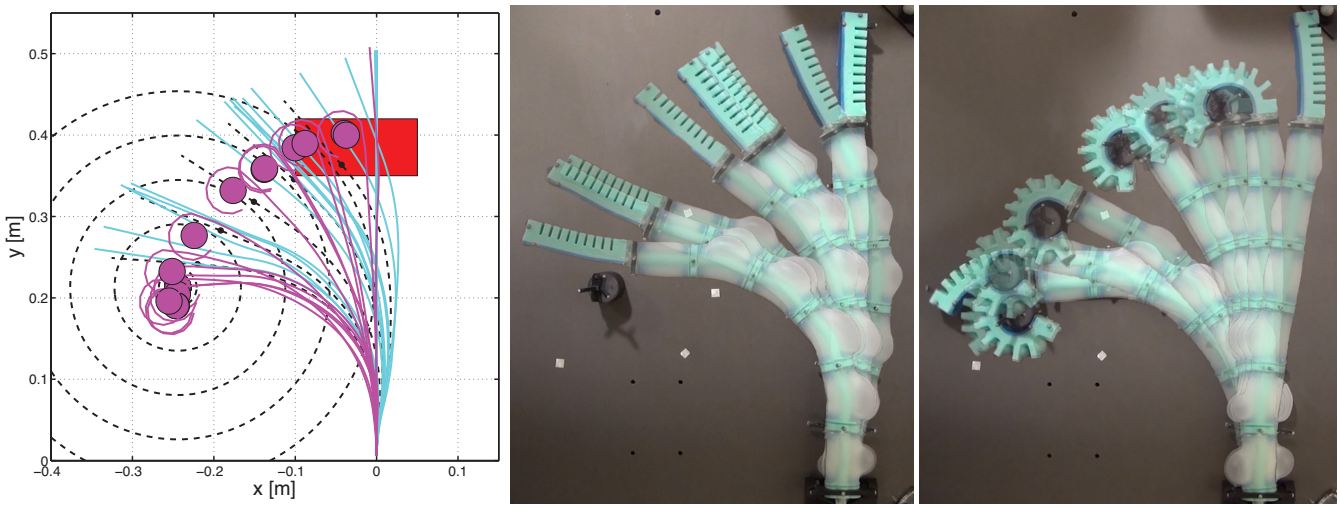

Figure 8: Left: A time series representation of an experimental grasp-and-place trial for an object located at point E (Figure 7). Here, the locally optimal planned manipulator configurations as well as planned sequential approach circles are shown as black dotted curves. The arm and gripper are shown in their experimentally determined configuration representations at 1 second intervals. The cyan configurations represent the manipulator prior to grasping the object, that is moving from its initial configuration to the object's location. Depending on where the object is placed, the manipulator takes between 17-35 s to approach it. After grasping the object, the magenta configurations represent the manipulator moving from the object's location back to the bin location shown in red. This task of moving back to the bin takes between 10-20 s. Right: Overlaid photographs of the manipulator moving from its initial pose to the object and from the object to the release location, respectively.

6 Conclusion

This work describes a planar soft manipulator capable of pick-and-place operations under high uncertainty in the position and shape of the object. A soft gripper was designed, fabricated, and combined with a previously developed soft robotic arm. It was then shown that a minimal strain and collision-free approach to an object of interest can be achieved by posing the grasp motion plan as a series of constrained nonlinear optimization problems.

The fabrication approach presented has potential to generalize beyond just the fabrication of a gripper. The new approach is advantageous because it allows for arbitrary designs of internal fluidic cavities and the casting of a homogeneous soft segment. It removes the need for laminating several separately casted parts together. Such a homogeneous soft segment would allow for better robot performance since it is less prone to manufacturing inconsistencies and rupture.

The manipulator is suitable to perform delicate tasks with low payloads, for example grasping objects that should not be squeezed and/or should not break during manipulation. The ability to successfully and repeatedly perform object manipulation using a fully soft, multiple degree of freedom arm suggests that despite their extreme compliance, soft robots are capable of reliable and robust object manipulation while simultaneously providing inherently safe interactions with the environment. We also demonstrated the manipulator's ability to autonomously grasp an object, which leads to many potential applications for full soft robotic manipulation. In a manufacturing setting, this could resemble a soft robot stretched widely to pick up objects situated at various locations. In a human-centric environment, soft arm grasping manipulation may enable soft robots to interact safely with humans. Future work will investigate the dexterity of the arm when approaching same object poses in various ways, just by changing the constraints and cost function when optimizing for the inverse kinematics solution. Integrating proprioceptive sensing within a multi-segment soft actuator will further improve the use of these manipulators in occluded environments.

ACKNOWLEDGMENTS

This research was conducted in the Distributed Robotics Laboratory at MIT with support from the National Science Foundation, grant numbers NSF 1117178, NSF IIS1226883, NSF CCF1138967, and National Science Foundation Graduate Research Fellowship Program, primary award number 1122374. We are grateful for this support.

References

[1] Eric Brown, Nicholas Rodenberg, John Amend, Annan Mozeika, Erik Steltz, Mitchell R Zakin, Hod Lipson, and Heinrich M Jaeger. Universal robotic gripper based on the jamming of granular material. *Proceedings of the National Academy of Sciences*, 107(44):18809–18814, 2010.

[2] M Calisti, A Arienti, ME Giannaccini, M Follador, M Giorelli, M Cianchetti, B Mazzolai, C Laschi, and P Dario. Study and fabrication of bioinspired octopus arm mockups tested on a multipurpose platform. In *Biomedical Robotics and Biomechatronics (BioRob), 2010 3rd IEEE RAS and EMBS International Conference on*, pages 461–466. IEEE, 2010.

[3] M Calisti, M Giorelli, G Levy, B Mazzolai, B Hochner, C Laschi, and P Dario. An octopus-bioinspired solution to movement and manipulation for soft robots. *Bioinspiration & biomimetics*, 6(3):036002, 2011.

[4] Jorge G Cham, Sean A Bailey, Jonathan E Clark, Robert J Full, and Mark R Cutkosky. Fast and robust: hexapedal robots via shape deposition manufacturing. *The International Journal of Robotics Research*, 21(10-11):869–882, 2002.

[5] Kyu-Jin Cho, Je-Sung Koh, Sangwoo Kim, Won-Shik Chu, Yongtaek Hong, and Sung-Hoon Ahn. Review of manufacturing processes for soft biomimetic robots. *International Journal of Precision Engineering and Manufacturing*, 10(3):171–181, 2009.

[6] Raphael Deimel and Oliver Brock. A compliant hand based on a novel pneumatic actuator. In *Robotics and Automation (ICRA), 2013 IEEE International Conference on*, pages 2047–2053. IEEE, 2013.

[7] Raphael Deimel and Oliver Brock. A novel type of compliant, underactuated robotic hand for dexterous grasping. In *Robotics: Science and Systems*, 2014.

[8] M.R. Dogar and S.S. Srinivasa. Push-grasping with dexterous hands: mechanics and a method. In *Intelligent Robots and Systems (IROS), 2010 IEEE/RSJ International Conference on*, pages 2123–2130, Oct 2010.

[9] Bianca Homberg, Robert K Katzschmann, Mehmet Dogar, and Daniela Rus. Haptic identification of objects using a modular soft robotic gripper. In *Intelligent Robots and Systems (IROS), 2015 IEEE/RSJ International Conference on*, Sept 2015.

[10] Koji Ikuta, Hironobu Ichikawa, and Katsuya Suzuki. Safety-active catheter with multiple-segments driven by micro-hydraulic actuators. In Takeyoshi Dohi and Ron Kikinis, editors, *Medical Image Computing and Computer-Assisted Intervention MICCAI 2002*, volume 2488 of *Lecture Notes in Computer Science*, pages 182–191. Springer Berlin Heidelberg, 2002.

[11] Filip Ilievski, Aaron D Mazzeo, Robert F Shepherd, Xin Chen, and George M Whitesides. Soft robotics for chemists. *Angewandte Chemie*, 123(8):1930–1935, 2011.

[12] Robert K Katzschmann, Andrew D Marchese, and Daniela Rus. Hydraulic Autonomous Soft Robotic Fish for 3D Swimming. In *2014 International Symposium on Experimental Robotics (ISER 2014)*, number 1122374, Marrakech, Morocco, 2014.

[13] Jinglin Li and Jing Xiao. A general formulation and approach to constrained, continuum manipulation. *Advanced Robotics*, 29(13):889–899, 2015.

[14] Andrew D Marchese, Robert K Katzschmann, and Daniela Rus. Whole arm planning for a soft and highly compliant 2D robotic manipulator. In *Intelligent Robots and Systems (IROS), 2014 IEEE/RSJ International Conference on*. IEEE, 2014.

[15] Andrew D. Marchese, Robert K. Katzschmann, and Daniela Rus. A recipe for soft fluidic elastomer robots. *Soft Robotics*, 2(1):7–25, 2015.

[16] Andrew D Marchese, Konrad Komorowski, Cagdas D Onal, and Daniela Rus. Design and control of a soft and continuously deformable 2d robotic manipulation system. In *Robotics and Automation (ICRA), 2014 IEEE International Conference on*. IEEE, 2014.

[17] Ramses V Martinez, Jamie L Branch, Carina R Fish, Lihua Jin, Robert F Shepherd, Rui Nunes, Zhigang Suo, and George M Whitesides. Robotic tentacles with three-dimensional mobility based on flexible elastomers. *Advanced Materials*, 25(2):205–212, 2013.

[18] Bobak Mosadegh, Panagiotis Polygerinos, Christoph Keplinger, Sophia Wennstedt, Robert F Shepherd, Unmukt Gupta, Jongmin Shim, Katia Bertoldi, Conor J Walsh, and George M Whitesides. Pneumatic networks for soft robotics that actuate rapidly. *Advanced Functional Materials*, 24(15):2163–2170, 2014.

[19] Panagiotis Polygerinos, Stacey Lyne, Zheng Wang, Luis Fernando Nicolini, Bobak Mosadegh, George M. Whitesides, and Conor J. Walsh. Towards a soft pneumatic glove for hand rehabilitation. In *Intelligent Robots and Systems (IROS), 2013 IEEE/RSJ International Conference on*, pages 1512–1517. IEEE, November 2013.

[20] Daniela Rus and Michael T Tolley. Design, fabrication and control of soft robots. *Nature*, 521(7553):467–475, 2015.

[21] Robert F Shepherd, Adam A Stokes, Rui Nunes, and George M Whitesides. Soft machines that are resistant to puncture and that self seal. *Advanced Materials*, 25(46):6709–6713, 2013.

[22] Erik Steltz, Annan Mozeika, Nick Rodenberg, Eric Brown, and Heinrich M Jaeger. JSEL: Jamming skin enabled locomotion. In *Intelligent Robots and Systems, 2009. (IROS) 2009. IEEE/RSJ International Conference on*, pages 5672–5677. IEEE, October 2009.

[23] Adam A Stokes, Robert F Shepherd, Stephen A Morin, Filip Ilievski, and George M Whitesides. A hybrid combining hard and soft robots. *Soft Robotics*, 1(1):70–74, 2014.

[24] Deepak Trivedi, Christopher D Rahn, William M Kier, and Ian D Walker. Soft robotics: biological inspiration, state of the art, and future research. *Applied Bionics and Biomechanics*, 5(3):99–117, 2008.

[25] Robert J Webster and Bryan A Jones. Design and kinematic modeling of constant curvature continuum robots: A review. *The International Journal of Robotics Research*, 29(13):1661–1683, 2010.

[26] Younan Xia and George M Whitesides. Soft lithography. *Annual review of materials science*, 28(1):153–184, 1998.

[27] Jing Xiao and Rayomand Vatcha. Real-time adaptive motion planning for a continuum manipulator. In *Intelligent Robots and Systems (IROS), 2010 IEEE/RSJ International Conference on*, pages 5919–5926. IEEE, 2010.